*G. Bolz* and G. Lange**

# Multiaxial Fatigue under Two-stage Block Loading

**REFERENCE** Bolz, G. and Lange, G., **Multiaxial fatigue under two-stage block loading**, *Multiaxial Fatigue and Design*, ESIS 21 (Edited by A. Pineau, G. Cailletaud, and T. C. Lindley) 1996, Mechanical Engineering Publications, London, 379–394.

**ABSTRACT** For a better understanding of variable amplitude multiaxial fatigue, interaction of two load stages is studied in the high-cycle fatigue range of the aluminium alloy 2017A–T4. In the first step the fatigue behaviour in constant amplitude tests is determined. In the second step lifetime and crack growth behaviour are studied in some sequential series of two multiaxial blocks with different load horizons and/or principal stress axes. Nucleation and growth of microcracks are investigated by microexamination of specimens and by using the replica technique. A significant influence of the anisotropic microstructure on crack propagation and lifetime was found. Well-mixed sequences of two multiaxial blocks result in lifetimes of 0.5 to 2.0 related to Miner's rule. Whereas uniaxial overloads had no influence, multiaxial overloads caused lifetimes of 0.3 to 7.0 times the linear value. The increased lifetimes are due to crack branching, crack path deviation or retardation of growth rate. The shorter lifetimes are due to reduced retardation effects at grain boundaries.

## 1 Introduction

In the last thirty years much effort has been made to research fatigue limit, lifetime and the cyclic behaviour of materials under constant amplitude multiaxial loading. Different kinds of damage parameters were defined, and up to now there is no agreement on whether to look for damage in the volume or on a critical plane.

In comparison only few examinations were made on the fatigue behaviour under variable amplitude multiaxial loading, most of them with two-stage tests (**1–5**), less with random- or incremental-step-tests (**6–8**). But the most important question for quantifying damage cycle by cycle with changing principal axes has not been addressed.

Crack growth under uniaxial variable amplitude loading is already a very complex process considering the closure of fatigue cracks due to overloads and changes in mean stress. In multiaxial variable amplitude loading, crack growth is additionally influenced by the interaction of the different crack planes cycle by cycle. The aspect of crack closure in the shear mode or in nonproportional mixed-mode loading has been been sufficiently examined (**8**).

This paper deals with the fatigue behaviour of the aluminium alloy 2017A–T4 under multiaxial two-stage block loading, where loads are limited to the range

*Technical University of Braunschweig, Langer Kamp 8, D-38106 Braunschweig, Germany.

of high cycle fatigue. Fatigue tests were carried out on thin-walled unnotched tube-like specimens under plane stress conditions, loaded by axial force and torsional moment. Experimental lifetimes are evaluated in relation to calculated lifetimes by the linear damage accumulation on the basis of constant amplitude $S/N$ curves for multiaxial loading. Special attention is given to the orientation and growth behaviour of the fatigue cracks within the anisotropic microstructure of the extruded material.

## 2 Material Specimen Geometry and Testing Device

The chemical composition and the mechanical properties of the investigated aluminium alloy 2017A (AlCuMg1) are given in Table 1 and Table 2, respectively.

**Table 1 Chemical composition of the alloy 2017A–T4 (weight percent)**

| | Si | Fe | Cu | Mn | Mg | Cr | Zn | Ti |
|---|---|---|---|---|---|---|---|---|
| *Measured* | 0.428 | 0.245 | 3.992 | 0.543 | 0.828 | 0.032 | 0.148 | 0.02 |
| DIN 1725 T1 | 0.2–0.8 | 0.7 | 3.5–4.5 | 0.4–1.0 | 0.4–1.0 | $\leqslant 0.1$ | $\leqslant 0.25$ | — |

**Table 2 Mechanical properties of the alloy 2017A–T4**

| | $R_m$ (MPa) | $R_{p0.2}$ (MPa) | $A_5$ (%) | HB 2.5/62,5/10 | $\sigma_w$ ($N_f = 10^5$) (MPa) | $\tau_w/\sigma_w$ ($N_f = 10^5$) |
|---|---|---|---|---|---|---|
| *Measured* (parallel axis) | 435 | 273 | 27,7 | 128 | 230 | 0.55 |
| *Measured* (hoop direct.) | 443 | 279 | 17,5 | 128 | 221 | — |
| DIN 1747 T1 | 380 | 260 | 10 | 110 | — | — |

The material was supplied in the form of hot-extruded rods with a diameter of 40 mm. It was solution-treated (150 min./500°C), quenched and naturally aged. Tubular specimens with wall thickness of 1.5 mm (Fig. 1a) were machined with an electropolished outer surface and a honed bore. The microstructure in the tubular area (Fig. 1b) shows an unrecrystallized extruded structure with a grain size of ca. 150 $\mu$m in radial and in hoop direction and a large size of more than 1 mm in axial direction.

Load controlled fatigue tests were performed on a servohydraulic testing machine (Schenck, axial force max. $\pm 100$ kN) with a supplemental torsional module (max $\pm$ 500 Nm) developed in our laboratory (description in (9)). External control of the load blocks was carried out by a personal computer. This facilitates the generation and control of any load–time function on both of the load axes independent of each other.

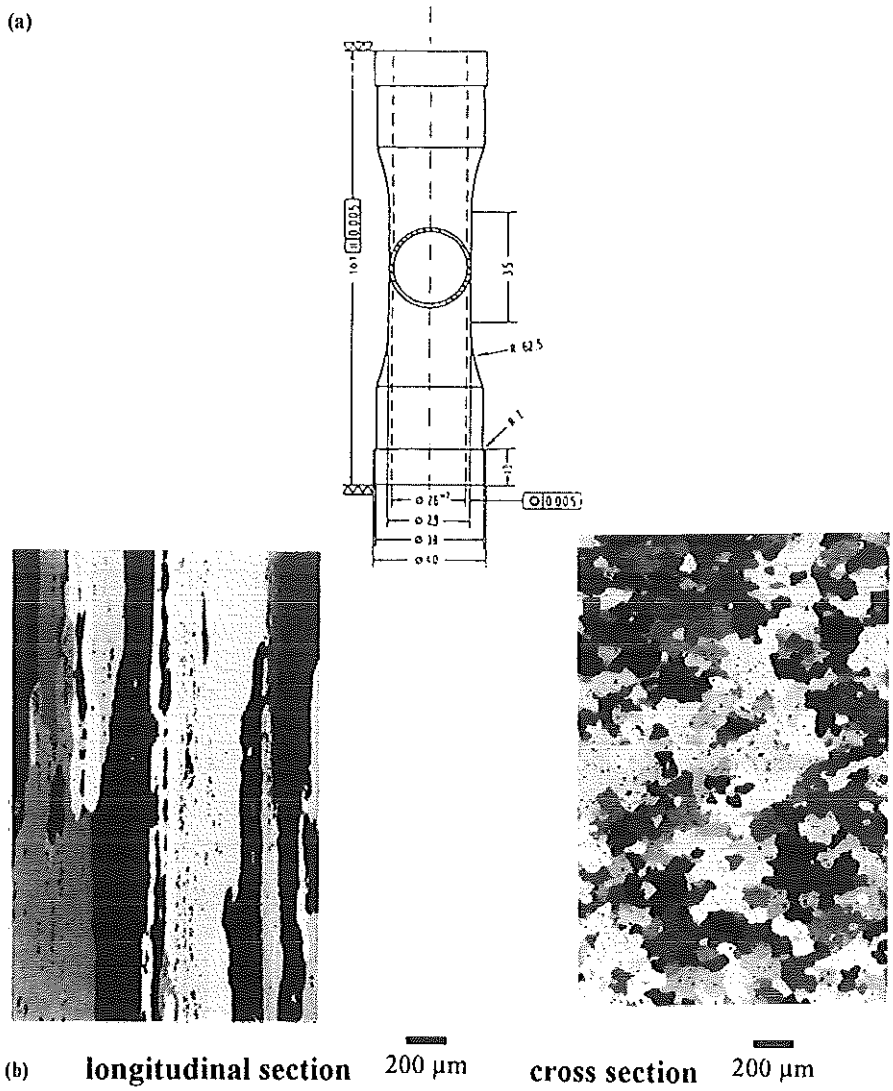


Fig 1 Specimen geometry (a) and microstructure (b).

## 3 Experimental Procedure

First of all basic S/N curves were determined for the load combinations given in Table 3 with 5 to 7 specimens on each load level. All time functions were sinusoidal with equal frequency of 10 Hz on axial force and torsional moment. Phase-shifted tests were carried out with a phase angle of 90 degrees for loading

with $R = -1$ and a phase angle of 180 degrees in loading with $R = 0$. For a better understanding of the parameters in the presented tests, the stress–time function of the two load axes in each block is given by an icon.

**Table 3 Basic uniaxial and multiaxial constant amplitude test**

| *Case of load* | *Relation* $\tau_a/\sigma_a$ | *Phase shift* $\alpha$ (deg.) | *Mean stress* $\tau_m$ (MPa) | *Mean stress* $\sigma_m$ (MPa) |
|---|---|---|---|---|
| | 0 | 0 | 0 | 0 |
| | 0 | 0 | 0 | $\sigma_a$ |
| | $\infty$ | 0 | 0 | 0 |
| | $\infty$ | 0 | $\tau_a$ | 0 |
| | 0.55 | 0 | 0 | 0 |
| | 0.55 | 90 | 0 | 0 |
| | 0.55 | 0 | $\tau_a$ | $\sigma_a$ |
| | 0.55 | 180 | $\tau_a$ | $\sigma_a$ |
| | 1.5 | 0 | 0 | 0 |
| | 1.5 | 90 | 0 | 0 |

Starting out from the multiaxial S/N curves, two load levels were defined for the two-stage tests: the first as the 'lower level' with a mean lifetime of 200 000 cycles to failure and the second as the 'higher level' with a mean lifetime of 40 000 cycles to failure.

Two different groups of two-stage loading were considered.

(1) A sequential change of the axes of principal stress (and/or the phase shift) and/or a change in the load level after equal sized blocks of 1 or 1000 cycles per block.
(2) A single multiaxial overload on the high level after each block of 100 cycles on the low level basic load.

The varied parameters included the relation $\tau_a/\sigma_a$, the phase shift $\alpha$, the mean stress ($\tau_m = 0$ or $\tau_m = \tau_a$, $\sigma_m = 0$ or $\sigma_m = \sigma_a$) and the load level. The completed two-stage fatigue tests contained a large number of possible test parameter combinations. Only a limited selection can be presented here.

Crack growth was investigated by the replication method, using thin sheets of cellulose acetate with a thickness of 35 $\mu$m. Fatigue cracks on both the replica and the failured specimen were examined by light-optical microscopy. This method is favourable to scanning-electron microscopy due to the greater contrast of fine cracks on the electropolished surfaces.

## 4 Results and Discussion

A better understanding of fatigue under two-stage block loading requires a knowledge of the general damage mechanisms in the investigated alloy under constant amplitude uniaxial and multiaxial loading. Some general features about

(a)

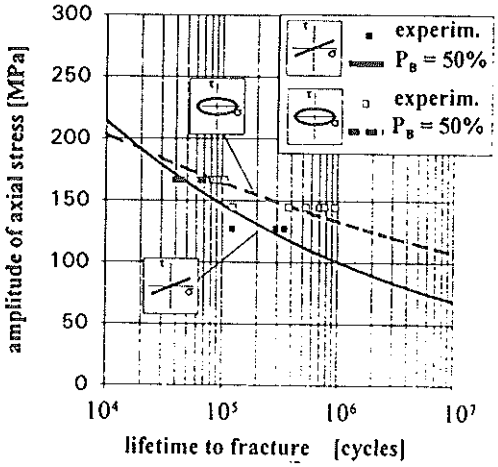


(b)

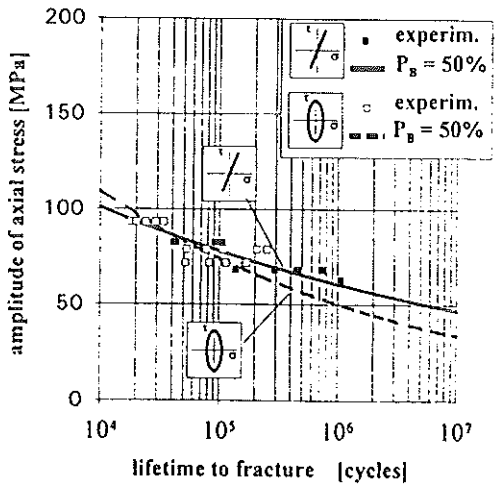


**Fig 2 S/N curves for biaxial constant amplitude loading: (a) $\tau_a/\sigma_a = 0.55$ and (b) $\tau_a/\sigma_a = 1.5$, phase shift 0 and 90°.**

initiation and growth of the fatigue cracks will be given at first, followed by the results of the basic constant amplitude tests and of the two-stage block series.

### 4.1 *General fatigue crack behaviour*

Crack initiation was observed in all cases to start on the outer electropolished surface by cracking of constituent particles of about 10 $\mu$m in size, by debonding of these particles or by impinging slip bands at the interface of the particles. On the high load level, microcracks with a length of only a few microns can be seen after the first cycles. On the low level, crack initiation takes about 30%

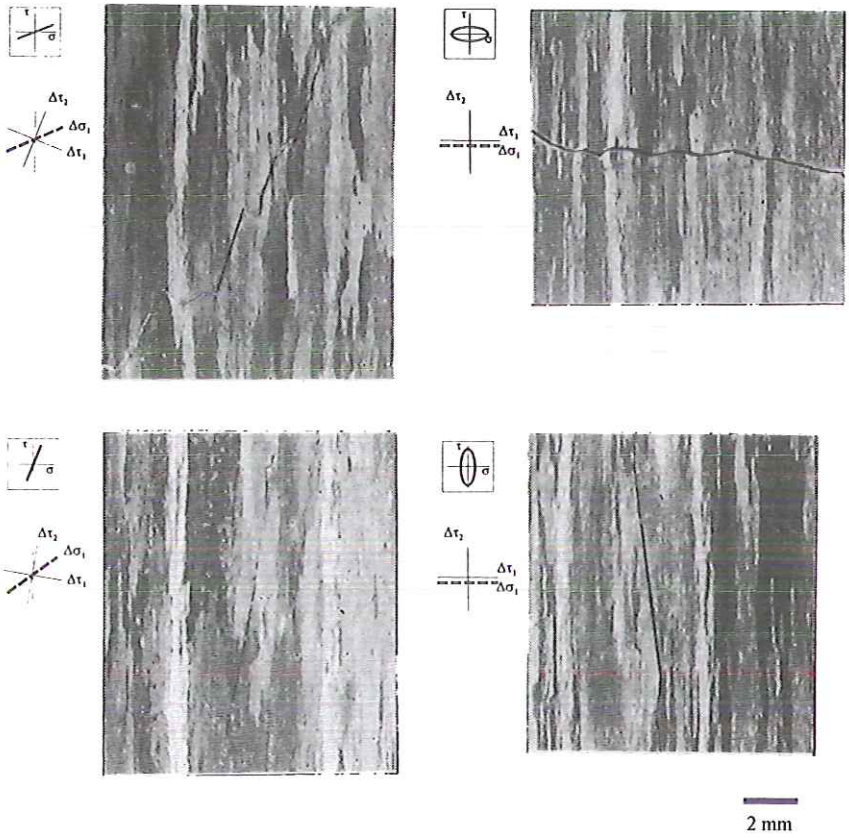


**Fig 3 Typical main cracks for biaxial constant amplitude loading.**

of lifetime. Crack growth continues from these initation sites on slip planes in Stage I for the greatest part of the life, except for pure axial loading and some two-stage tests, where propagation turns into Stage II after 50 to 80% of life.

The fatigue cracks show a thumbnail shape in the beginning and grow along the surface in mixed case A. Only in uniaxial loading some case B cracks were observed. Failure takes place shortly after the crack breaks through the specimen wall (1.5 mm thickness). Then the crack has a surface length of only a few millimetres, and the crack growth becomes unstable. This is equal to a crack tip loading in the order of the fracture toughness of the alloy. This failure criterion was taken for all tests.

### 4.2 *Constant amplitude tests*

Figure 2 shows the S/N curves for alternating loading with $\tau_a/\sigma_a = 0.55$ and $\tau_a/\sigma_a = 1.5$, each with a phase shift of 0° and 90°, respectively. In Fig. 3 the

typical cracks for the four types of loading are shown. Under the loading with $\tau_a/\sigma_a = 0.55$ the crack plane turns from $\sim 20°$ to the specimen axis in the synchronous case into a plane perpendicular to the tubular axis in the nonproportional case. The higher number of grain boundaries in this direction, which the crack has to cross, may cause the higher lifetime. In the case of loading with $\tau_a/\sigma_a = 1.5$ the phase shift leads to a reduction in lifetime compared with the proportional loading. In both loadings the fatigue cracks grow on a plane at a small angle to the specimen axis. The phase-shifted loading favours crack growth on a plane parallel to the tubular axis. In this direction the fatigue cracks need only cross a couple of grains to get the critical size for failure.

In proportional loading, crack planes obviously consist of a number of crystallographic facettes (**10**) in uniaxial tests on a naturally aged AlCu–4 alloy. In nonproportional loading, crack growth is determined by shearing too, but in the case of $\tau_a/\sigma_a = 0.55$, facetting is not the main mechanism and noncrystallographic crack growth is observed.

The results show that the influence of a phase shift cannot generally be described only by a material constant, as mentioned in recent studies. In addition, special attention has to be given to the microstructure.

A study of crack growth was made by the replication method on at least one specimen of each loading case of Table 3. Crack growth was determined by projection of the real crack length onto the plane of maximum shear stress amplitude. The effective cyclic stress intensity factor was calculated from a von Mises' type equation

$$\Delta K_{\text{eff}} = \sqrt{(\Delta\sigma_{\text{eff}}^2 + 3\Delta\tau_{\text{eff}}^2)\pi a}$$

with the half crack length $a$, the effective normal stress range $\Delta\sigma_{\text{eff}} = \sigma_{\max} - \sigma_{\text{closure}}$ and the effective shear stress range $\Delta\tau_{\text{eff}}$. Crack closure was assumed for $\sigma = 0$; $\Delta\tau_{\text{eff}}$ is taken as the full range of shear stress on the plane of maximum shear stress amplitude.

The measured crack growth rates are shown for the main cracks in alternating uniaxial and multiaxial loading in Fig. 4. Some drops in the growth rate nearly up to the critical value of $\Delta K_{\text{eff}}$ of 30 MPa$\sqrt{\text{m}}$ show that there is short crack behaviour over most of the lifetime. The slope of the Forman-type line is very small with a value of 1.5. This means that growth rates are high compared to long cracks at low values of stress intensity factors. The reduction of the growth rate above $\Delta K_{\text{eff}} > 10$ MPa$\sqrt{\text{m}}$ can be related to the turn from Stage I to Stage II. This was observed by Akiniwa *et al.* (**11**), who made a statistical analysis of the short crack behaviour in smooth specimens of 2024–T3 under uniaxial alternating loading.

### 4.3 *Two-stage block tests*

Only a small selection with characteristic results will be presented here. For a better evaluation of the experimental lifetimes, it is favourable to look at those

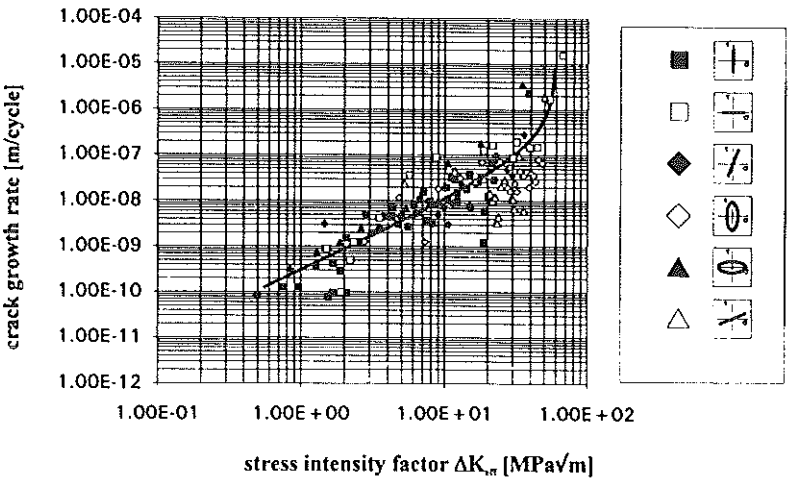


**Fig 4 Crack growth rate in constant amplitude alternating loading.**

values that are related to the calculated lifetimes from Miner's rule with the base on the S/N curves from multiaxial constant amplitude tests.

*Sequential change between equal sized blocks*

These tests were carried out to determine how damage develops when the stress state is changed sequentially after blocks of a certain number of cycles. The chosen block sizes with 1 cycle per block represent an immediate load change and those with 1000 cycles per block a quasi-constant loading within each block and less sequential influence.

Figure 5 shows the lifetime results of a selection of the test series. The loading in the two blocks of each series can be taken from the icons. A weight at the bottom is the sign for the low-load level, the weight on top for the high level, respectively. All lifetimes (related to Miner's rule) of the performed test series in this group are in the range of 0.5 to 2.0. This is in good agreement with the linear damage rule with the value of 1.0. No characteristic influence of block size or a change in the load level, in the relation $\tau_a/\sigma_a$, or in the phase shift $\alpha$ was deducible.

The present results have to be compared with lifetimes from equivalent studies from the literature. In one of the earlier investigations on this topic, McDiarmid (1) carried out tests on tubular specimens of the aluminium alloy BS 2L65 under synchronously combined stresses in longitudinal and hoop direction with block sizes of $10^3$ to $10^5$ cycles. These results are in a comparative range with values related to Miner's rule of 0.13 to 1.82, despite the test series with high hoop stresses which lead to the very short lifetimes of 0.13.

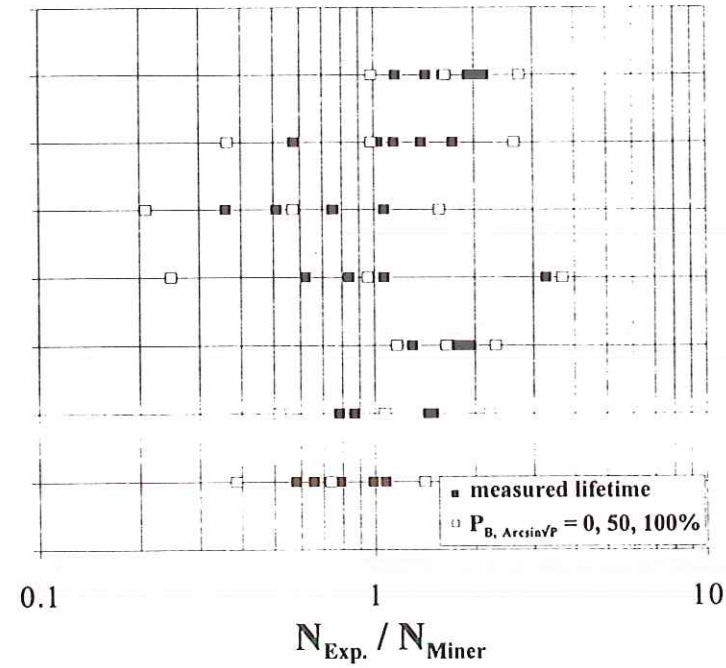


**Fig 5 Lifetimes of a selection of two-stage block loading with equal sized blocks of 1 or 1000 cycles per block.**

Tests on steel XC18 with a sequential load change from bending to torsion cycle-by-cycle or in equal sized blocks of $10^4$ cycles were performed in the range of high cycle fatigue by Lasserre and Froustey (**5**). They found lifetime values little higher than predicted by Miner's rule.

From the pure aspect of lifetime, the linear damage rule describes the results of the very simple two-stage tests in a satisfactory manner, compared with uniaxial random tests. It has to be kept in value of the linear calculation. Special interest must be given to the background of experimental lifetimes by investigating the damage mechanisms due to fatigue cracks.

In the tested material, cracks usually grow in Stage I up to the critical crack length for failure. In the two-stage tests, the same behaviour was observed. Some features of the main cracks are given in Fig. 6. In series with misorientated preferred crack planes – as in the simple example of a sequential change from tension to torsion (Fig. 6a) – crack growth may only happen in one of the two blocks (in Fig. 6a only in torsion). This results in a related lifetime of the order of 2.0. A small angle between the preferred crack planes of the blocks will yield cracks like those found in constant amplitude tests (Fig. 6b). In this case the damage sums are of the order of 1.0 or below. A test series with two phase-shifted blocks (block 1 with $\tau_a/\sigma_a = 0.55$ and block 2 with $\tau_a/\sigma_a = 1.5$, both on the low

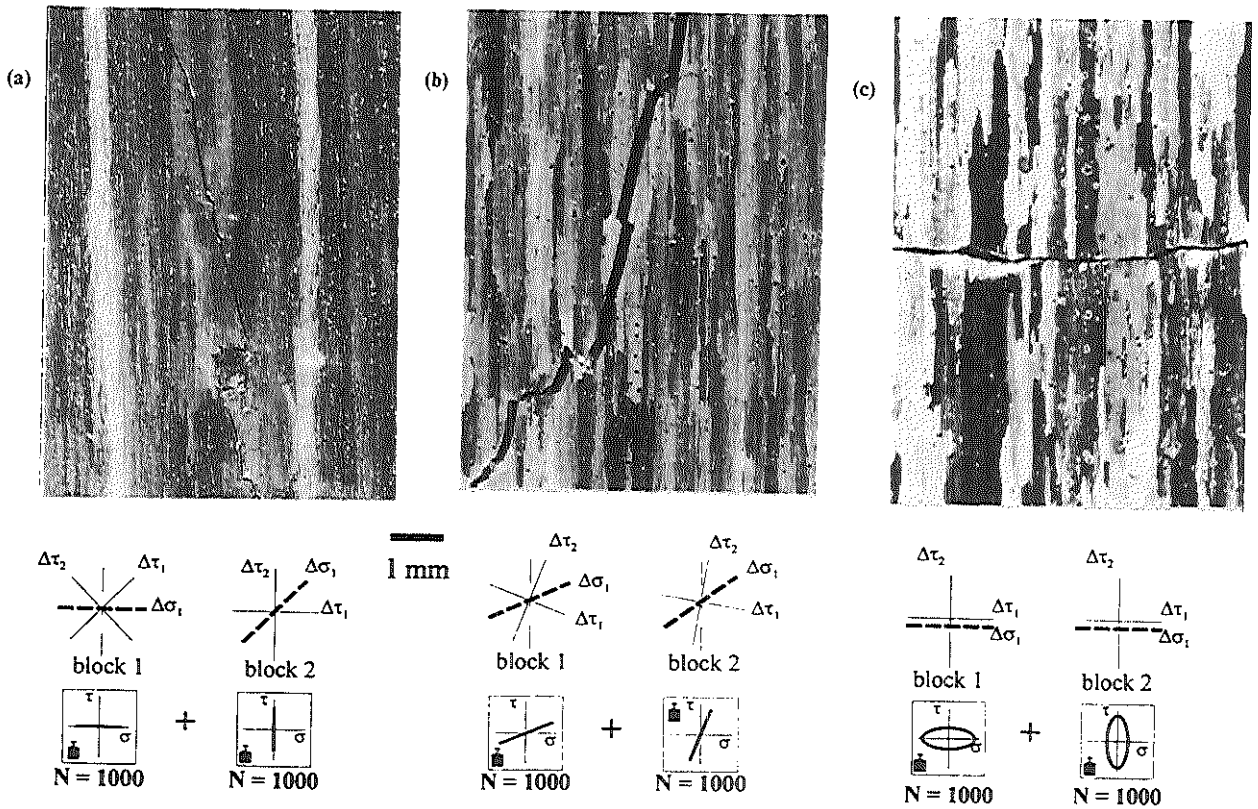


Fig 6 Selection of main cracks in two stage block loading with equal sized blocks.

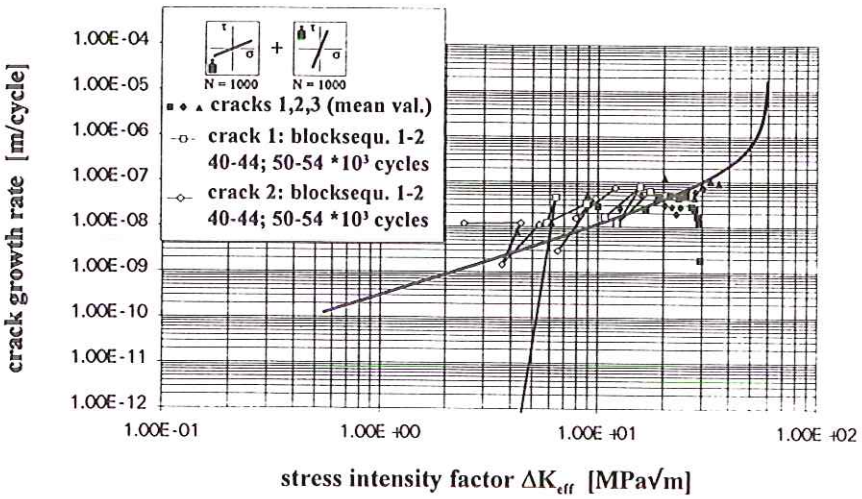


**Fig 7 Crack growth rate in a two-stage block loading with equal sized blocks.**

level) causes higher lifetimes by a position of the main crack perpendicular to the specimen axis (Fig. 6c).

The crack growth rate of one test series with equal sized blocks of 1000 cycles is shown in Fig. 7. The mean propagation rate is of the order of the Forman-type curve from the constant amplitude tests. Short crack behaviour is observed up to failure. The measuring points for the crack growth during one block lie within the scattering band.

*Single overload after each block of 100 cycles on the base level*

The aim of this part of the presented research was to get information about the damage development when there is a constant amplitude base level which is interrupted by single loads of a higher amplitude. These contribute negligibly to the damage sum in the linear calculation. All the loadings were limited to the load range of high cycle fatigue. The base level was chosen as the 'low level' with a constant amplitude lifetime of 200 000 cycles. The overload was of the 'high level' with 40 000 cycles to failure. This 'overload' has only an amplitude of about 20% above the base level.

Uniaxial block sequences of this type (torsion or tension) cause lifetimes of the order of the linear rule. This is in good agreement with the uniaxial fracture mechanics research by Stephens *et al.* (**12**) on the aluminium alloy 2024–T3. The main question is, whether multiaxial overloads have an influence on lifetime within high cycle fatigue or not.

Figure 8 shows a selection of lifetime results of multiaxial test series with overloads, in relation to Miner's rule. Though the overloads are within range

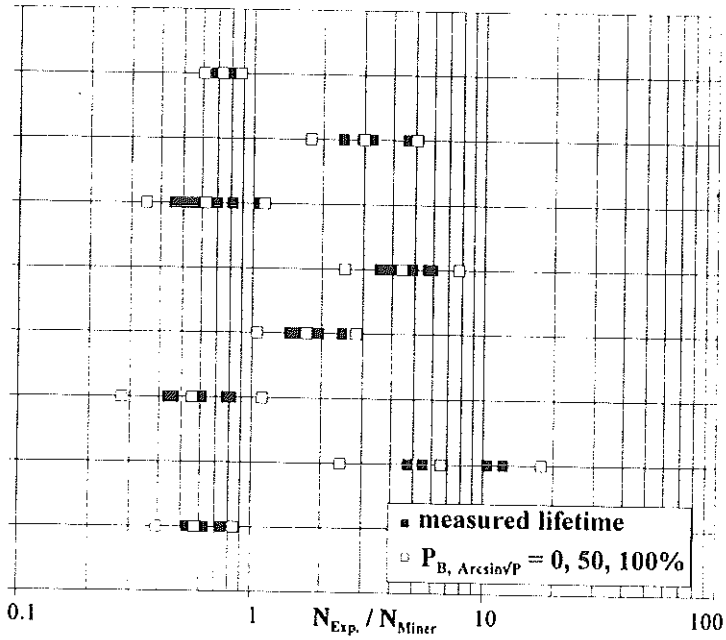


**Fig 8 Lifetimes of a selection of two-stage block loading with single overload after each block of 100 cycles on the base level.**

of high cycle fatigue, their effect on lifetime is obvious: the mean lifetimes range from 0.3 to 7.0.

From uniaxial tests it is known that overloads influence the crack growth rate by crack tip hardening and crack closure. The multiaxial tests show some additional effects, which may cause the misfit to Miner's rule.

- crack branching;
- forcing an early change to noncrystallographic growth in Stage II;
- turning the crack angle in relation to the microstructure;
- reducing the drop in crack growth rate at grain boundaries;
- retarding the crack, by crack tip hardening.

A very simple example for an increase of lifetime by crack branching is the sequence with torsion at base level and an overload of tension (Fig. 9a). The usual straight crack in the direction of the tubular axis has branched. This results in a lifetime of 4.6 times the linear calculation. In constant amplitude loading the synchronous load case with $\tau_a/\sigma_a = 0.55$ causes Stage I cracks on the plane of maximum shear stress. The synchronous mixed-mode overload

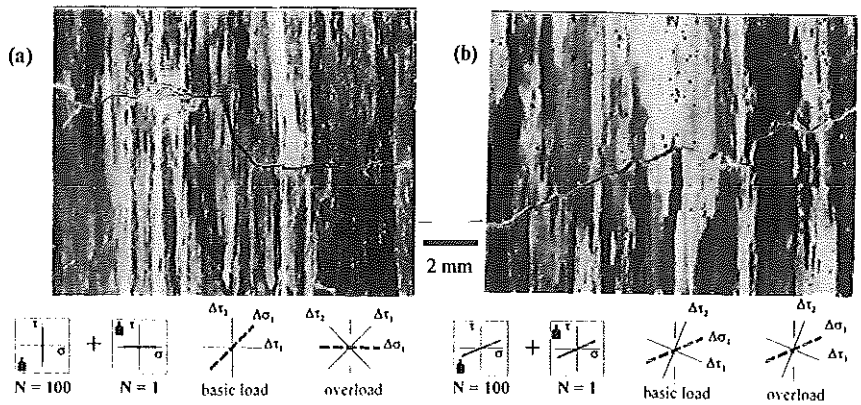


**Fig 9 Main cracks in two-stage blockloading with single overload after each blockof 100 cycles on the base level: branched crack (a), stage II crack (b).**

with the same relation of $\tau_a/\sigma_a$ forces an early change into Stage II crack growth (Fig. 9b) and increases the lifetime to about 3 times the linear calculated value.

Even when the increased lifetime can be interpreted by the changed crack paths, this does not explain the very short or the very long lifetimes. The answer is given by the examination of the crack growth rates by the replication method. Figure 10 shows the crack growth rates for two series with phase-shifted base load and phase-shifted overload, both in the alternating load range. The only difference between the two series is the change in the relation of $\tau_a/\sigma_a$ (Fig. 10a: base level $\tau_a/\sigma_a = 0.55$, overload $\tau_a/\sigma_a = 1.5$; Figure 10b: base level $\tau_a/\sigma_a = 1.5$, overload $\tau_a/\sigma_a = 0.55$). The growth rate in Fig. 10a lies continuously above the Forman curve from the constant amplitude tests. The absence of any drop in the growth rate leads to the shorter related lifetime of 0.5. The opposite happens in the series of Fig. 10b. The maximum values are below the Forman curve and all the crack stop in the range of $\Delta K_{eff}$ equals 10 to 20 $MPa\sqrt{m}$. The result is a mean lifetime within this series of 7.0 times the linear calculated lifetime.

The effects of higher mixed-mode overloads on crack growth were studied with CT specimens of AlZnMgCu 1.5 by Henn (**13**) and with 4-point bending specimens of 4340 steel by Nayeb–Hashemi (**14**). The results of both authors correspond in the fact that mode II overloads have no significant effect on subsequent mode I crack growth, but mode I overloads cause significant crack retardation.

The crucial topic for further research is to find a method of damage evaluation in multiaxial variable-amplitude loading. One question is whether damage should be calculated on a critical plane, as discussed by Bannantine and Socie

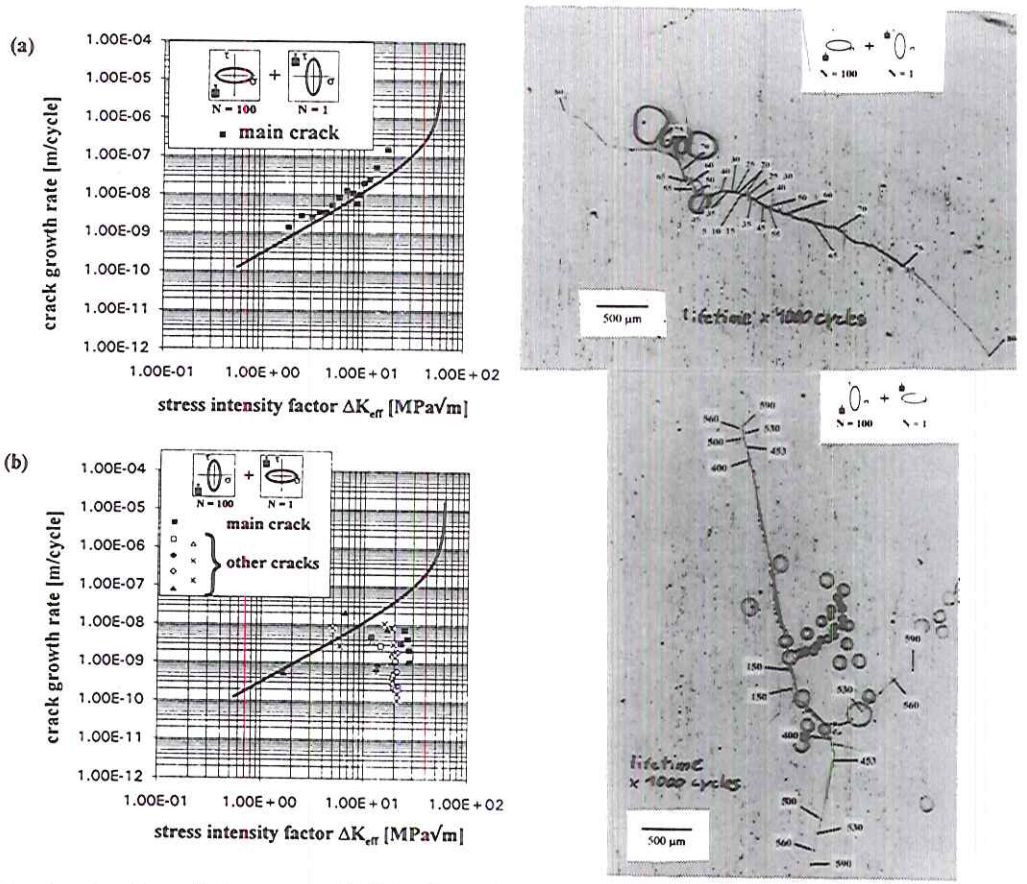


Fig 10 Crack growth rate and main cracks in two-stage block loading with single overload, when lifetime is extremely reduced (a) or increased (b).

(9), or with damage parameters for each cycle, as carried out by Sanetra (7) or Prochotta (8). Special attention should be given to the fracture mechanics approach, but much work must be done in future to achieve a reliable calculation of lifetime including nonproportional loading.

## 5 Conclusions

Crack growth in the present alloy is strongly influenced by the large-grained anisotropic microstructure and shows short crack behaviour up to the critical crack length. Therefore the results cannot be generalized for other materials.

(1) Lifetime of multiaxial two-stage loading in high-cycle fatigue depends on the interaction of the preferred crack growth planes of each block.
(2) Multiaxial overloads or alternating blocks with different shear planes can reduce crack retardation at grain boundaries compared with uniaxial loading.
(3) Longer lifetimes compared with Miner's rule have their origin in unfavourable related crack growth planes of the two blocks. Especially phase-shifted overloads can force much longer lifetimes by a general retardation of the propagation rate, when uniaxial loading has no influence.
(4) A reliable lifetime prediction for multiaxial service loading has to take the additional influence of the microstructure into account, especially when the axes of principal stress are variable.

## References

(1) McDIARMID, D. L. (1974) Cumulative damage in fatigue under multiaxial stress conditions, *Proc. Instn. Mech. Engrs.* **188**, (40), pp. 423–430.
(2) HUG, J., LIU, J., SCHRAM, A., ZENNER, H. (1993) Einfluß der Mehrachsigkeit auf die Ribbildung und ausbreitung bei schwingender Beanspruchung, **25**, *Vortragsveranstaltung des DVM–Arbeitskreises Bruchvorgänge*, Karlsruhe, Febr. 16/17, 1993, pp. 59–74.
(3) ROBILLARD, M., CAILLETAUD, G. (1989) Directionally defined damage in multiaxial low cycle fatigue: experimental evidence and tentative modelling, *3rd Int. Conf. on Biaxial/Multiaxial Fatigue*, Stuttgart, April 3-6, 1989.
(4) HARADA, S., ENDO, T. (1989) On the validity of Miner's rule under linearly combined loading of rotating bending and cyclic torsion, *3rd Int. Conf. on Biaxial/Multiaxial Fatigue*, Stuttgart, April 3-6, 1989.
(5) LASSERRE, S., FROUSTEY, C. (1992) Multiaxial fatigue of steel – testing out of phase and in blocks: validity and applicability of some criteria, *Int. J. Fatigue*, **14**, (2), pp. 113–120.
(6) SANETRA, C., ZENNER, H. (1989) Multiaxial fatigue under constant and variable amplitude loading, *3rd Int. Conf. on Biaxial/Multiaxial Fatigue*, Stuttgart, April 3-6, 1989.
(7) BANNANTINE, J. A., SOCIE, D. F. (1989) A variable amplitude multiaxial fatigue life prediction method, *3rd Int. Conf. on Biaxial/Multiaxial Fatigue*, Stuttgart, April 3-6, 1989.
(8) PROCHOTTA, J. (1991) Verhalten kurzer Risse in Stählen bei biaxialen Betriebsbelastungen, Diss. RWTH Aachen.
(9) RODE, D., LANGE, G. (1988) Beitrag zum Ermüdungsverhalten mehrachsig beanspruchter Aluminiumlegierungen, *METALL*, **42**, (6), pp. 582–587.
(10) BRETT, S. J., CANTOR, B. and DOHERTY, R. D. (1977) *Proc. 4th Int. Conf. Fracture*, Waterloo, Bd. 2, pp. 719–723.
(11) AKINIWA, Y., TANAKA, K., MATSUI, E. (1988) Statistical characteristics of propagation of small fatigue cracks in smooth specimen of aluminium alloy 2024–T3, *Mat. Science Engineering*, **A104**, pp. 105–115.

(12) STEPHENS, R. I., CHEN, D. K., HOM, B. W. (1976) Fatigue crack growth with negative stress ratio following single overloads in 2024–T3 and 7075–T6 aluminium alloys, in *ASTM STP*, **595**.

(13) HENN, K. (1990) Ein Beitrag zur Lebensdauervorhersage von Bauteilen mit Rissen, Diss, Univ. Kaiserslautern.

(14) NAYEB-HASHEMI, H. (1989) Effects of Mode I and Mode II overloads on subsequent Mode I crack growth in AISI 4340 steels, (M. W. Brown, K. J. Miller, Edts) *Biaxial and Multiaxial Fatigue*, EGF 3, London: Mechanical Engineering Publications, pp. 265–283.